Allostery in *Callinectes sapidus* Hemocyanin: Cooperative Oxygen Binding and Interactions with L-Lactate, Calcium, and Protons†

B. A. Johnson,‡ C. Bonaventura, and J. Bonaventura*

Marine Biomedical Center, Duke University Marine Laboratory, Beaufort, North Carolina 28516

Received July 8, 1987; Revised Manuscript Received November 17, 1987

ABSTRACT: Allosteric interactions of *Callinectes sapidus* hemocyanin have been investigated by generation of precision oxygen-binding curves using a modified Imai apparatus and their subsequent analysis using numerical methods. The Monod–Wyman–Changeux (MWC) model, the MWC model extended to include hybrid R_3T_3 states, and the phenomenological Adair equation were fit to the experimental data. The hybrid MWC model provided a quantitatively better fit to the data than did the MWC model. The fits of the hybrid model and the Adair equation were statistically similar, supporting the adequacy of the hybrid model as a description of cooperative oxygen binding by *C. sapidus* hemocyanin. The hybrid model is also supported by an apparent negative cooperativity at the fourth oxygen-binding step, a feature that is not possible with the conventional MWC model. The oxygen-binding curves obtained at various concentrations of three allosteric effectors, Ca, protons, and L-lactate, were analyzed in terms of the hybrid MWC model. All three effectors altered both the affinities of the model states and the equilibrium constants between the states. L-Lactate, which increases affinity and decreases cooperativity, increased the affinity of both the R and T states as well as preferentially stabilizing the hybrid and R states. Protons, which decrease affinity and cooperativity, act by reducing the affinity of both the R and T states and stabilizing the R state. Ca ions, which increase both affinity and cooperativity, act by increasing the affinity of the R state and preferentially stabilizing the T state.

Hemocyanins are large, extracellular, oxygen-transport proteins that reversibly bind oxygen at an active site comprised of paired copper atoms. Homotropic allosteric interactions are manifested as cooperative oxygen binding. Heterotropic allosteric interactions are manifested as an altered oxygen affinity in the presence of both organic (e.g., L-lactate) and inorganic (calcium, protons, etc.) ions. Models of the oxy and deoxy forms of the active site have been used to explain the observed alterations in oxygen affinity during both the homotropic and heterotropic allosteric interactions (Bonaventura et al., 1982; Solomon, 1981; van Holde & Miller, 1982). However, because the specific geometry of the active site is still controversial, acceptance of any structural model for the allosteric interactions has been precluded. Furthermore, as interactions among the active sites must be communicated via changes in protein conformation, the formulation of specific mechanistic models will not be feasible until substantial progress is made in the development of a high-resolution three-dimensional model of both oxy and deoxy states of the protein [see, however, Gaykema et al. (1986)].

Mathematical models, however, can be effective in interpreting function and in guiding the development of experiments aimed at elucidating both the structure and function of proteins. Analysis of oxygen equilibrium data by mathematical modeling can suggest the presence of different affinity states within distinct, structural states. The two-state allosteric model of Monod, Wyman, and Changeux (MWC) (1965) has been found adequate to describe hemoglobin oxygenation under any single condition. The two-state model is inadequate, however, to describe the results from changing the concentrations of allosteric effectors (Imai, 1982). As shown by Imai (1982), models that allow for states having affinities different from either the T or R state result in a better fit to the data despite the observation of only two distinct structural states by X-ray crystallography. These results suggest that subtle structural changes may result in states of altered affinity.

Numerical analysis of oxygen equilibrium curves can be performed in terms of a phenomenological equation such as the Adair equation, which gives information about oxygen-binding affinities at each step and also about the number, affinity, and sequence of binding of allosteric effectors (Brouwer, 1982a). Analysis can also be performed in terms of a model equation, such as the original or extended MWC models, that yields information about the change in equilibria between states. If changes in the affinity of the states are observed, additional states in the model may be needed (Minton & Imai, 1974).

As with hemoglobin, most attempts to model the function of hemocyanin begin with the two-state model of Monod, Wyman, and Changeux (1965). With some hemocyanins modifications of the MWC model have been found to be necessary to describe oxygen equilibrium curves adequately. The binding of oxygen to hemocyanin from *Limulus polyphemus*, for example, can be described by the MWC model only if the affinity of the deoxygenated molecule is allowed to vary in the presence of allosteric effectors (Brouwer et al., 1977). In the analysis of oxygen-binding behavior of hemocyanin from *Penaeus* (Brouwer et al., 1978) and *Callianassa* (Miller & van Holde, 1974), the affinity of the R and T states could be held constant, but the existence of a hybrid state having three subunits in the R state and three subunits in the T state had to be postulated. The reader is referred to the Appendix for a more detailed description of the extended (hybrid) MWC model.

† This work was supported in part by National Science Foundation Grant DMB-8309857 and National Institutes of Health Grant ESO-1908 to J.B. and C.B. and NSF and James B. Duke Graduate Fellowships to B.A.J.

‡ Present address: Merck, Sharp and Dohme Research Laboratories, P.O. Box 2000, Rahway, NJ 07065-0900.

0006-2960/88/0427-1995$01.50/0

The above conclusions about the adequacy of various models of hemocyanin function are largely based on visual impressions of the fit between experimental data and a theoretical curve. It is difficult to make quantitative conclusions in this manner. Decker et al. (1983) have introduced a graphical test for the MWC model, but this technique also does not allow for quantitative conclusions. We adapted the experimental technique of Imai (1981), which is capable of producing precise and complete oxygen equilibrium curves, to the measurement of hemocyanin–oxygen-binding curves. Numerical techniques were then used for the analysis of the resulting curves. Specifically, curves have been generated for *Callinectes sapidus* hemocyanin in various concentrations of allosteric effectors. These curves have been fit, where possible, to the phenomenological Adair equation and to the original and the extended (hybrid) MWC model. As will be shown, the extended MWC model is quantitatively adequate to describe the curves. The unmodified two-state model yields fits that are statistically significantly poorer. Data are presented on the interactions of L-lactate, calcium, and protons with the protein. We show that these effectors alter hemocyanin function in complex and dissimilar ways, altering both the affinities of the R and T states and the equilibrium between the R, T, and hybrid states.

Experimental Procedures

Hemocyanin was prepared from the hemolymph of the blue crab as described earlier (Johnson et al., 1984). Separation of the dodecameric fraction was accomplished by gel filtration on Fractogel 55S as described by Johnson (1987). Except where noted, experiments reported are based on purified preparations of the dodecameric form. Native preparations used consist of approximately 80% dodecamers and 20% hexamers. It was found that the inclusion of the hexameric fraction does not result in appreciable change in the qualitative or quantitative results reported herein.

All oxygen equilibrium curves were performed at 20 °C in an automated Imai cell (Johnson, 1984). The curves were generated in the presence of 15 mM 4-(2-hydroxyethyl)-1-piperazineethanesulfonic acid (Hepes) buffer with approximately 90 mM Cl^-. Calcium titration experiments were done at constant chloride concentration.

The theoretical equations described in the Appendix were fit to the data with a nonlinear, least-squares regression program (Johnson et al., 1981). The data were weighted during the fitting process as described by Imai (1982). The Adair equation was fit by using intrinsic k_i terms in order that the program would provide confidence intervals for these parameters. The fit was comparable when it was done in terms of overall equilibrium parameters. The statistical significance of the improvement in fit obtained by extending the original MWC model to include the hybrid state was tested by using the criterion of Mannervik (1982). The sums of the squared residuals for the two models are compared by calculating the quotient

$$(SRS_o - SRS_e)(n - p_e)/(p_e - p_o)SRS_e \qquad (1)$$

The number of data points is n, the number of parameters in the original model is p_o (=5) and includes the absorbances in the presence and absence of oxygen as floatable parameters, and the number of parameters in the extended model is p_e (=6). The sum of squared residuals for the two models is SRS_o and SRS_e. If quotient 1 is greater than the F-statistic $F(p_e-p_o, n-p_e)$, then the extension to the original model is warranted.

The above criterion is applicable if the two models to be compared are similar. This similarity is seen in the comparison of the original MWC model with the hybrid MWC model, since the latter consists of the simple addition of one parameter to the original model.

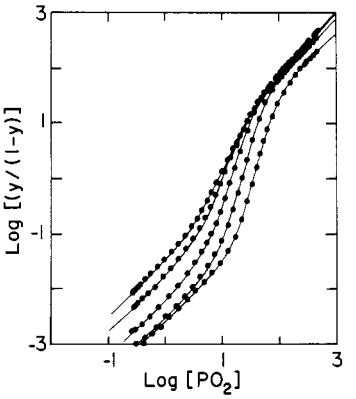

FIGURE 1: Hill plots of oxygen equilibrium curves of native *C. sapidus* hemocyanin in 15 mM Hepes buffer, 20 °C, with 83 mM NaCl, pH 7.56. Lactate concentrations are 0, 1.0, 4.0, 16.0, and 50.0 mM, increasing from right to left. Solid lines are best fit to the hybrid MWC model.

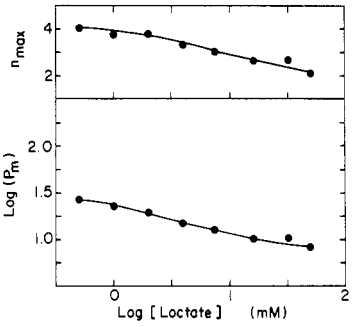

FIGURE 2: Effect of L-lactate on the affinity and cooperativity of *C. sapidus* hemocyanin. Conditions as in Figure 1.

Where two models are essentially different, as in the Adair equation and the hybrid MWC model, the above criterion is not valid. In such cases Mannervik (1982) has found that if the number of data points is greater than 15, an alternative method is acceptable. In this case the statistical significance of the differences in fit of the two models to the data is tested by calculating the quotient

$$\frac{SRS_o/(n - p_o)}{SRS_e/(n - p_e)} \qquad (2)$$

If this quotient is greater than 1.5, then the model with the higher variance is rejected.

Results and Discussion

Allosteric Effects of L-*Lactate, Calcium, and Protons.* As we described earlier (Johnson et al., 1984), L-lactate increases the oxygen affinity of *C. sapidus* hemocyanin. An extensive data set on oxygen binding by *Callinectes* hemocyanin was collected to facilitate analysis under varied conditions and evaluation according to the proposed mathematical models. Figure 1 shows a series of Hill plots at concentrations of L-lactate from 0 to 50 mM. A plot of the median ligand affinity, P_m, and the slope of the Hill plot, N_{max}, as functions of L-lactate concentration is shown in Figure 2. Under the lower ionic strength conditions used in this set of experiments, the change in affinity is greater than that reported in our earlier paper. In the present experiments L-lactate at a concentration of 10 mM reduced the log P_{50} by 0.49 unit, as compared to the change of 0.28 unit found in the earlier experiments. We consider it probable that the anions (Cl^- in particular) present in the artificial seawater solution used in

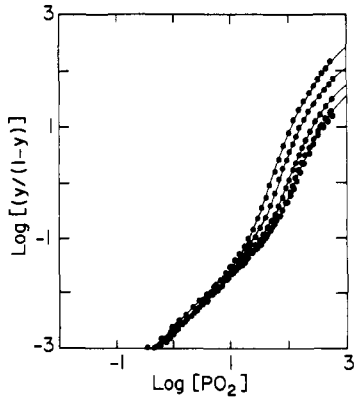

FIGURE 3: Effect of calcium on the Hill plot of the *C. sapidus* oxygen equilibrium curve at pH 7.01 in 15 mM Hepes buffer. Total chloride concentration was maintained at 103 mM by addition of NaCl. Ca concentrations are 0.105, 0.56, 1.0, 4.0, 16.0, and 50.0 mM, increasing from right to left. Solid line is best fit to hybrid MWC model.

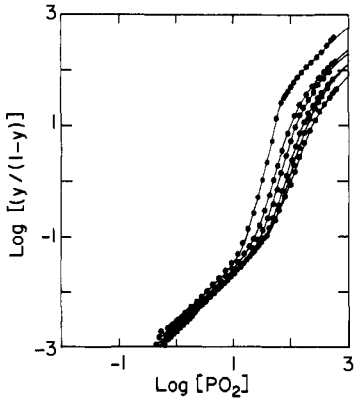

FIGURE 4: Effect of calcium on the Hill plot of the *C. sapidus* oxygen equilibrium curve at pH 7.55 in 15 mM Hepes buffer. Total chloride concentration was maintained at 103 mM by addition of NaCl. Ca concentrations are 0.3, 1.0, 2.0, 4.0, 8.0, and 16.0 mM, increasing from right to left. Solid line is best fit to hybrid MWC model.

the earlier experiments compete with the L-lactate anion for the binding site. Experiments designed explicitly to test this hypothesis were not carried out. However, analysis of the effect of L-lactate on the P_m* as done in Johnson et al. (1984) indicates that the apparent affinity of the sites for L-lactate is approximately 10 times higher in the present set of data for which the dissociation constant is 0.22 mM and 65% confidence intervals are 0.16–0.31 mM. The confidence intervals for the number of lactate binding sites are overlapping for the two sets of data.

Calcium, a divalent cation, interacts with *C. sapidus* hemocyanin and increases both the oxygen affinity and the cooperativity as shown in Figures 3–5. The results shown are very similar to those previously reported by Brouwer et al. (1983). These results are not in agreement with the conclusions reached by Mason et al. (1983), who report no effect of calcium on the cooperativity of oxygen binding by *C. sapidus* hemocyanin.

Brouwer et al. (1983) demonstrated the existence of 2.4–3.0 high-affinity (dissociation constant, 11–25 μM) and 14–42 low-affinity calcium binding sites (dissociation constant 1–5 mM) in each hexamer. The experiments of Brouwer et al. (1983) suggested that the effect of calcium on oxygen affinity was a result of interaction at the low-affinity sites. The effect on the cooperativity reported by these authors, however, was more pronounced at lower calcium levels, suggesting that this effect was related to the high-affinity calcium binding sites. Experiments for the present study were performed to provide

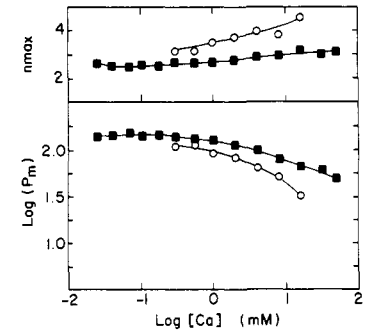

FIGURE 5: Effect of calcium on the affinity and cooperativity of *C. sapidus* hemocyanin. Conditions as in Figures 3 and 4. (■) pH 7.01; (○) pH 7.55.

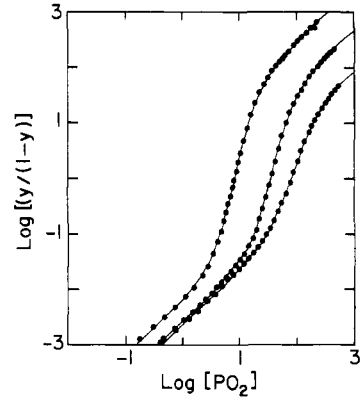

FIGURE 6: Effect of pH on the Hill plot of the *C. sapidus* oxygen equilibrium curve in 15 mM Hepes buffer with 10 mM $CaCl_2$ and 83 mM NaCl. The pH is 7.14, 7.61, and 8.18, increasing from right to left. Solid line is best fit to hybrid MWC model.

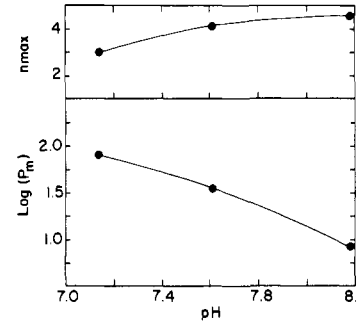

FIGURE 7: Effect of pH on the affinity and cooperativity of *C. sapidus* hemocyanin. Conditions as in Figure 6.

more data at low calcium levels in order to test this difference. We found, however, that neither cooperativity nor affinity was significantly changed at calcium levels below approximately 0.3 mM. Analysis of the effect of Ca on P_m, in the manner used for the lactate analysis, indicates the existence of 1.8 (65% confidence intervals are 1.6–2.0) sites per hexamer, with a dissociation constant (oxyhemocyanin) of 1.4 mM at pH 7.01 (65% confidence intervals are 1.0–1.9). At pH 7.55, there are 4.3 sites per hexamer (confidence intervals 3.5–5.4), with a dissociation constant from oxyhemocyanin of 3 mM (confidence intervals 2–6). From their affinities we conclude that these oxygen-linked sites correspond to the low-affinity sites measured by Brouwer et al. (1983). The number of sites determined here, which correspond only to oxygen-linked sites, is much smaller than the total number of sites they measured. This difference indicates that many of the calcium binding sites do not affect the binding of oxygen.

Figures 6 and 7 illustrate the increase in affinity and cooperativity that occurs as the pH is raised from 7.1 to 8.1. The

Table I: Comparison of Fits to Original and Extended (Hybrid) MWC Models

pH	model[a]	log $P_{50,R}$	log $P_{50,T}$	log L	log Q	rms[b]
7.14	O	1.28	2.63	3.8		0.005
	H	0.9	2.65	5.7	1.0	0.001
7.61	O	0.48	2.54	6.4		0.007
	H	0.25	2.59	7.8	1.5	0.002
8.18	O	−0.33	2.13	7.5		0.05
	H	−0.48	2.21	8.4	1.6	0.002

[a] O, original (two-state) MWC model; H, hybrid MWC model. [b] Root mean square deviation between experimental data and fitted equation. Within each data set all variances are statistically, significantly, different ($P > 0.999$). Data are from the same experiments as Figure 6.

value of the Bohr effect (0.9) is somewhat smaller than the value (1.2) reported for the artificial seawater experiments of our earlier paper (Johnson et al., 1984) but is very similar to that reported by Mason et al. (1983).

Comparison of Models of Allostery. A comparison of the ability of the original and extended MWC models (see Appendix) to describe the oxygen equilibrium curve of *C. sapidus* was made by numerically fitting the data from each of several curves to both models. A comparison of the two models at three pHs is shown in Table I. At all pHs the decrease in variance resulting from the additional parameter of the extended model is statistically significant at a probability level greater than 0.999. Thus, the extended (hybrid) model provides a better description of the experimental data, confirming the conclusions reached in other studies of crustacean hemocyanins (Miller & van Holde, 1974; Brouwer et al., 1978).

The above analysis indicates that the extended (hybrid) model provides a better description of the experimental results than does the original MWC model. It is possible, however, that another model might provide yet a better fit to the data. This was tested by comparing the fit of the extended (hybrid) MWC model with the fit of the Adair equation. Since the Adair equation is a phenomenological equation, making no assumption about any underlying structural features and being capable of describing any pattern of oxygenation, it provides a standard against which other models can be compared. Other models may work as well as the Adair equation, but none should work better.

The comparison to the Adair equation is, however, made more complex by two factors. First, fitting data to the Adair equation, particularly the six-site model, is very difficult. Often least-squares fitting routines are unable to converge on a set of parameters that minimize the estimated variance [even for a four-site model (Mills, 1978)]. Convergence was obtained, however, in many of the experimental data sets that were

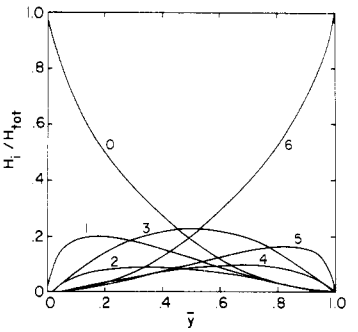

FIGURE 8: Fractional population of the different liganded species as a function of average ligation state. *C. sapidus* hemocyanin measured at pH 8.18 in 15 mM Hepes buffer with 10 mM $CaCl_2$ and 83 mM NaCl.

attempted. Second, since the Adair equation and the extended (hybrid) MWC model are not simply interconvertible by addition or subtraction of terms and the statistical test employing quotient 1 is thus not valid, the less rigorous test based on quotient 2 was used.

The root mean square deviation obtained in the fit of the extended (hybrid) MWC model and the Adair equation to a variety of experimental data sets are shown in Table II. The ratio of the variances, quotient 2, is less than 1.5 in all but one case, and there the discrepancy is minor. Thus, both models can be considered to fit the data equally well. This is strong evidence to support the adequacy of the extended (hybrid) MWC model as a descriptor of oxygen binding by the hemocyanin of *C. sapidus*.

Additional insight into the changing oxygen affinity of the hemocyanin during the cooperative oxygen-binding process can be obtained by calculating the values of the association constants at each oxygen-binding step. These are the Adair parameters, and they can be obtained either by fitting the Adair equation to the data or by calculating them from the parameters obtained by fitting the extended (hybrid) MWC model to the data. While the values of the parameters calculated by the two methods are not in exact agreement, in most cases they are quite close (Table II). A most important feature is that k_4 is actually lower than k_3 for some of the data sets. The decrease in the Adair constant is an expression of an apparent negative cooperativity at this step, a feature that is not describable by the original MWC model. As shown in the Appendix, the extended (hybrid) model is capable of describing this type of negative cooperativity, thus providing further strong support for its use.

By using the Adair parameters, it is possibile to calculate the fractional population of the different ligation states of the hemocyanin as a function of average saturation with oxygen.

Table II: Comparison of the Fit of Oxygen Equilibrium Data from *C. sapidus* to the Adair Model and the Hybrid MWC Model[a]

	Adair constants with data set[b]								
model	1	2	3	4	5	6	A_{min}	A_{max}	rms[c]
A	0.0018	0.0028	0.004	0.017	0.02	0.16	0.1552	1.049	0.0005
H	0.0018	0.0021	0.009	0.007	0.03	0.14	0.1552	1.048	0.0005
A	0.0025	0.007	0.00	0.3	0.02	0.9	0.2396	1.1579	0.0018
H	0.0025	0.004	0.05	0.0	0.14	0.5	0.2396	1.1593	0.0014
A	0.0371	0.008	1	0.01	0.7	0.65	0.226	1.1358	0.0019
H	0.0312	0.044	0.1	0.10	0.1	0.78	0.227	1.1353	0.0013
A	0.002	0.006	0.002	0.0	0.02	0.12	0.1549	1.1120	0.0010
H	0.002	0.003	0.012	0.0	0.04	0.10	0.1549	1.1120	0.0034
A	0.0064	0.004	1.2	0.03	1.0	3.1	0.15635	1.1810	0.0017
H	0.0061	0.012	0.4	0.04	1.0	3.0	0.15637	1.1811	0.0019

[a] Number of digits shown determined by confidence limits from fit to the Adair equation. Data are from the same experiments as Figures 1, 4, and 6. Data set 1, Figure 4, 0.56 mM $CaCl_2$; data set, Figure 1, 0 mM L-lactate; data set 3, Figure 1, 50 mM L-lactate; data set 4, Figure 6, pH 7.14; data set 5, Figure 6, pH 8.18. [b] A, curve fit to Adair equation; H, curve fit to hybrid MWC model. [c] Root mean square deviation between experimental data and fitted equation.

Table III: Effect of Calcium, L-Lactate, and pH on the Parameters of the Hybrid MWC Model and on the Median Ligand Affinity

effector	model parameter[a]				
	log $P_{50,R}$	log $P_{50,T}$	log L	log Q	log P_m
lactate (pH 7.56)	−0.2*	−0.5*	−0.8*	−0.9*	−0.3*
pH (pH 7.55)	−1.4*	−0.3*	3.3*	0.6*	−0.9*
Ca (pH 7.01)	−0.5*	0	1.5*	−0.2	−0.2*
Ca (pH 7.55)	−0.7*	−0.2	1	0.9*	−0.3*

[a] An asterisk indicates that the slope of the regression of log parameter vs log effector is significantly different from zero.

Cooperative oxygen binding is normally reflected as a reduction in intermediate species. Figure 8 clearly shows that while the population of species with two or four ligands is reduced, a significant amount of hemocyanin with three ligands bound is found through much of the range. This can be readily interpreted as a reflection of the stability of the hybrid state, with a drop in affinity at the fourth ligation step.

It is important to note that this modeling of *C. sapidus* hemocyanin with the hybrid hexamer model holds true for pure preparations of dodecamers. This result and the similarity of oxygen affinities and cooperativities of dodecamers and hexamers (Brouwer et al., 1982b) suggest that cooperative interactions in *C. sapidus* hemocyanin occur only within the hexameric substructure. Thus, our analysis of high-resolution data from oxygen equilibrium experiments suggests that the dodecameric hemocyanin of this crab consists of independently acting hexamers and that within each hexamer there are trimers which act semiindependently.

Allosteric Effects on Model Parameters. The above considerations indicate that the extended (hybrid) MWC model provides an excellent description of the oxygen equilibrium curves of *C. sapidus* hemocyanin at a given effector concentration. How are the parameters of this model influenced by the three allosteric effectors studied? In the context of either the original or extended MWC models, the allosteric effectors are generally described as affecting the oxygen equilibrium curve by shifting the equilibrium between the R and T states (that is, by changing the parameter L). Effectors that raise the affinity do so by stabilizing the R state, that is, by decreasing the value of L. Effectors that lower the affinity do so by stabilizing the T state, that is, by increasing the value of L.

If the affinities of the R and T states are constant, then a plot of the Hill coefficient as a function of log P_{50} should be an inverted parabola that intercepts the $n_h = 1$ line at log P_{O_2}, corresponding to the affinity of the R state and at log P_{O_2}, corresponding to the affinity of the T state. This is true for the hemocyanin from the ghost shrimp *Callianassa californiensis* (Miller & van Holde, 1974) and from the shrimp *Penaeus setiferus* (Brouwer et al., 1978). The data of this study, when plotted in such a manner (not shown), clearly do not fit such a pattern.

Allosteric effectors must interact with hemocyanin from *C. sapidus* by changing the affinities of the R and T states in addition to modifying the allosteric equilibrium constant. Indeed, the effect of pH, L-lactate, and calcium on the oxygen equilibria of hemocyanin from *C. sapidus* is to alter all of the parameters in a complex way. This complexity is apparent from studying Figures 1, 3, 4, and 6. The different patterns of shifts of the asymptotes of the oxygen equilibrium curves suggest that each effector shows a unique pattern of binding to the different states *Callinectes* hemocyanin.

The influence of the allosteric effectors on the parameters of the hybrid model can be expressed in a quantitative manner. Table III shows the results obtained from regressions of the logarithm of each parameter vs the logarithm of the effector concentration. The effect of both Ca and pH was dependent on the Ca concentration and pH. The reported values in Table III are at 10 mM calcium for both the pH and calcium effect and at pH 7.55 for the pH effect.

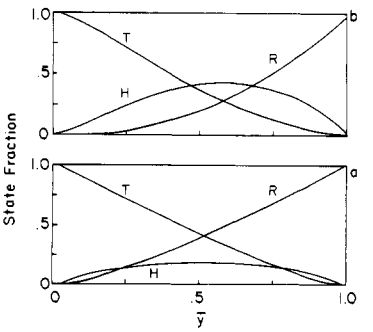

FIGURE 9: Fractional population of the R, T, and hybrid states as a function of fractional saturation in the absence (a) and presence (b) of 50 mM L-lactate.

The affinities of the R and T states of *Callinectes* hemocyanin are clearly affected by lactate concentration. The effect is greater on the T state, where the shift is approximately 3 times greater than that for the R state. This is rather unusual in that this effector raises the oxygen affinity of the protein and binds preferentially to the R state of the protein, as reflected in its effect on the oxygen pressure required for half-saturation and on the calculated allosteric equilibrium constant L (Table III). L-Lactate also clearly affects the equilibrium between the R and hybrid states (lowers Q).

Addition of L-lactate has a strong stabilizing effect on the population of the hybrid state where three subunits are in the R state and three are in the T state. The stabilization of the hybrid state can be illustrated by calculating the fraction of hemocyanin molecules in the three different states. Equations 3–5, allow these fractions to be calculated.

$$\bar{R} = \frac{(1+\alpha)^6}{(1+\alpha)^6 + L(1+c\alpha)^6 + 2(L/q)^{1/2}(1+\alpha)^3(1+c\alpha)^3} \quad (3)$$

$$\bar{T} = \frac{L(1+c\alpha)^6}{(1+\alpha)^6 + L(1+c\alpha)^6 + 2(L/q)^{1/2}(1+\alpha)^3(1+c\alpha)^3} \quad (4)$$

$$\bar{H} = \frac{2(L/q)^{1/2}(1+\alpha)^3(1+c\alpha)^3}{(1+\alpha)^6 + L(1+c\alpha)^6 + 2(L/q)^{1/2}(1+\alpha)^3(1+c\alpha)^3} \quad (5)$$

The results have been plotted as a function of the fractional saturation with oxygen and are shown in Figure 9. A comparison of parts a and b of Figure 9 shows that the hybrid state is much more populated at most oxygen levels in the presence of L-lactate.

Table III shows that the affinities of both the R and T states are reduced by the addition of protons. In this case the effect is greater on the R state. The equilibria both between the R and T states and between the R and hybrid states are also shifted by pH. While both increased L-lactate and pH raise the affinity of the protein for oxygen, their effects on cooperativity of oxygen binding are opposite. This result must in part be explained by the large stabilization of the T state relative to the R state (increased L), resulting from increased pH on the one hand and the large stabilization of the hybrid and R states by L-lactate on the other.

Calcium acts to raise the oxygen affinity of *Callinectes* hemocyanin. The effect on affinity is manifested as an increase

Table IV: Binding of Effectors at Each Oxygen Ligation Step

effector	Δ log k_i/Δ log effector						
	1	2	3	4	5	6	total
Ca (pH 7.01)	0.05	0.15	0.53	0.02	0.21	0.49	1.45
Ca (pH 7.55)	0.24	0.23	0.58	0.43	0.96	1.07	3.51
L-lactate (pH 7.56)	0.60	0.47	0.05	0.44	0.02	0.01	1.59
$[H^+]$ (pH 7.55)	−0.30	−0.41	−1.38	−0.38	−1.27	−1.45	−0.51

Table V: Relation among the Adair Parameters and the Parameters of the Original and Extended (Hybrid) MWC Equation[a]

	MWC	hybrid MWC
a_1	$(Lc + 1)/(D_1P_{50,R})$	$[H(c + 1) + Lc + 1]/(D_2P_{50,R})$
a_2	$(Lc^2 + 1)/(D_1P_{50,R}^2)$	$[H(2c^2 + 6c + 2) + 5(Lc^2 + 1]/(5D_2P_{50,R}^2)$
a_3	$(Lc^3 + 1)/(D_1P_{50,R}^3)$	$[H(c^3 + 9c^2 + 9c + 1) + 10(Lc^3 + 1)]/(10D_2P_{50,R}^3)$
a_4	$(Lc^4 + 1)/(D_1P_{50,R}^4)$	$[H(4c^3 + 12c^2 + 4c) + 10(Lc^4 + 1)]/(10D_2P_{50,R}^4)$
a_5	$(Lc^5 + 1)/(D_1P_{50,R}^5)$	$[H(5c^3 + 5c^2) + 5(Lc^5 + 1)]/(5D_2P_{50,R}^5)$
a_6	$(Lc^6 + 1)/(D_1P_{50,R}^6)$	$[2Hc^3 + Lc^6 + 1]/(D_2P_{50,R}^6)$

[a] $a_1 = k_1$, $a_2 = k_1k_2$, etc. $D_1 = L + 1$. $D_2 = 2H + L + 1$.

in the affinity of the R state. There is no effect on the affinity of the T state at pH 7.01, and the effect at pH 7.44 is not statistically significant (Table III). Even though the affinity of the hemocyanin is raised by Ca, the low-affinity T state is stabilized as shown by the increase in L, the allosteric equilibrium constant. At pH 7.5 some decrease in the stability of the hybrid state relative to the R state is also evident.

Sequence of Effector Binding. The sequence of effector binding to the hemocyanin is dependent on the type of effector. This can be seen more clearly by calculating the binding of allosteric ligands at each step of oxygenation. This can be calculated from the change in the value of each association constant of the Adair equation, resulting from a change in effector concentration:

$$\Delta \log k_i/\Delta \log \text{effector}$$

The derivatives corresponding to this equation were calculated from the slope of the regression of log k_i versus log effector. For this purpose k_i was derived from the extended (hybrid) MWC model by use of the parameter relationships shown in Table V. A plot of log k_i versus log E for calcium or protons is curved, indicating that the number bound at each step is dependent on the effector concentrations. The slopes were calculated at [Ca] = 10 mM, pH 7.55. Table IV shows the results of these calculations.

In total, approximately 1.6 molecules of L-lactate per hexamer are bound in going from the completely deoxygenated state to the completely oxygenated state. This number agrees well with the number of L-lactate binding sites calculated earlier (Johnson et al., 1984). Approximately equal increases in lactate binding are observed at the first, second, and fourth steps of oxygenation, with smaller increments of cofactor binding at the other steps. This result is consistent with the ability of lactate to increase the oxygen-binding affinity of the T state (Table III). Conversely, the binding of Ca is largest at the third, fifth, and sixth steps, consistent with its major effect on the oxygen affinity of the R state. The pattern of proton release is similar to that of calcium binding. The greatest changes occur at the third, fifth, and sixth steps.

Conclusions

L-Lactate, calcium, and pH alter the affinity and cooperativity of *C. sapidus* hemocyanin. Their effects are a result of a complex set of interactions with the protein. It is, unfortunately, not possible to describe all the various interactions as being due to shifts in the equilibrium between two discrete states of the protein having different affinities for the oxygen, as is done with the original MWC model. It has been suggested that in cases such as this, where clear changes in the apparent affinities of the R and T states occur, it is necessary to presume the presence of additional states of the protein (Minton & Imai, 1974). These researchers found that the interaction of effectors with hemoglobin could only be described by postulating the existence of a third state and suggested that it was inappropriate to analyze binding curves with the two-state model. Such an approach has recently been used for hemocyanin (Richey et al., 1985) and may be necessary to describe the varied allosteric interactions in *C. sapidus* hemocyanin. Such a model would probably require at least two additional states, each with hybrids possible among all the different states. The complexity of such a model would substantially reduce its heuristic value. Accordingly, and given the low resolution of structural knowledge about *C. sapidus*, we have not yet attempted to formulate such a model. Instead, for any given condition we have postulated the existence of R and T states with discrete affinities and shown the improvement of data fit that occurs within this context when allowance is made for a hybrid state in which three subunits of the hexamer assume the R state and the remaining three assume the T state. It should be emphasized that even the continuous distribution model proposed by Kotani (1968) that allows for an infinite number of states cannot describe the type of negative cooperativity seen in the oxygen equilibria of *C. sapidus* hemocyanin (Imai, 1982). As pointed out above, this can be satisfactorily explained by the hybrid model. Other alternatives to the use of the multistate model would be either of two recently developed models, the cooperon model (Coletta et al., 1986) or the nested model (Decker et al., 1986). We are currently examining the ability of the cooperon and nested models to adequately describe the oxygen-binding data described in this paper.

Existence of the hybrid states will only be proven, of course, when a suitable physical technique for demonstrating their existence is developed. The results of this paper, however, are consistent with the existence of such hybrid conformations and suggest conditions under which their concentrations are maximal.

Appendix

The MWC model is expressed mathematically by

$$y = \frac{\alpha(1 + \alpha)^5 + Lc\alpha(1 + c\alpha)^5}{(1 + \alpha)^6 + L(1 + c\alpha)^6} \quad \text{(A1)}$$

The ratio of the oxygen affinity in the two states is c:

$$c = P_{50,R}/P_{50,T} \quad \text{(A2)}$$

The oxygen concentration is expressed as a dimensionless parameter by multiplying by k_R:

$$\alpha = P_{O_2}/P_{50,R} \quad \text{(A3)}$$

The allosteric equilibrium constant (L) describes the equilibrium between the R and the T states in the absence of oxygen:

$$L = [T]/[R] \quad (A4)$$

While the original MWC model has successfully been used to describe the oxygen equilibrium curves of hemoglobin, it is inadequate to describe the oxygen equilibrium of hemocyanin from some arthropods. An extension to the original model has been found to describe the oxygen-binding data better for the hemocyanins from two species of crustacea (Miller & van Holde, 1974; Brouwer et al., 1978). The extension involves a modification of the requirement that the protein retains its symmetry during the conformational transition. In the extended model the protein is allowed to exist in a third state, which is a hybrid of the R and T states. In the hybrid state three subunits are in the low-affinity T state and three subunits are in the high-affinity R state. The two structural trimers that compose the hemocyanin hexamer may correspond to the functional trimers of the hybrid. The hybrid model is expressed mathematically as

$$y = \{\alpha(1+\alpha)^5 + Lc\alpha(1+c\alpha)^5 + (L/Q)^{1/2}[\alpha(1+\alpha)^2(1+c\alpha)^3 + c\alpha(1+\alpha)^3(1+c\alpha)^2]\}/\{(1+\alpha)^6 + L(1+c\alpha)^6 + 2(L/Q)^{1/2}[(1+\alpha)^3(1+c\alpha)^3]\} \quad (A5)$$

Q is related to the equilibrium between the hybrid and R state:

$$2(L/Q)^{1/2} = [H]/[R] \quad (A6)$$

From either version of the MWC model it is possible to calculate the intrinsic affintiy of oxygen binding at each ligand-binding step. These are the parameters ($k_1 \ldots k_6$) of the Adair equation. They are calculated by expanding the polynomials in the numerator and denominator of eq A1 or A5, collecting terms in equal powers of P_{O_2}, and comparing these term by term to the Adair equation. Table V shows the equivalences among these parameters.

A measure of the change in affinity can be obtained by comparing the difference between the association constants at successive steps of oxygen binding:

$$k_i - k_{i-1} = D \quad (A7)$$

In general, the Adair equation parameters can have any nonzero values, and hence D can be positive, negative, or zero. However, when calculated from the original MWC model, the Adair parameters must increase monotonically at each step. That is, negative cooperativity is not possible. Examination of the Adair parameters calculated from the extended MWC model, however, shows that an apparent negative cooperativity is possible with this model. This apparent negative cooperativity manifests itself as a drop in the association constant of the fourth site relative to the third. It is, however, more an expression of the semiindependence of the two trimers than a reduction in the affinity of the fourth site as a result of binding oxygen at the previous sites.

Substitution of the appropriate terms from Table V for the Adair constants (for the third and fourth steps, for example) for the hybrid model into eq A7, setting $D = 0$ and rearranging in terms of H ($H = L/Q$), yields

$$-[c^6 + 2c^5 + 3c^4 - 12c^3 + 3c^2 + 2c + 1]H^2 - 20[-Lc^6 + Lc^5 + Lc^4 - (L+1)c^3 + c^2 + c - 1]H + 100[Lc^4 - 2Lc^3 + Lc^2] = 0 \quad (A8)$$

At this value of H, ligand binding at these steps is noncooperative. Lower values of H yield positive cooperativity, while higher values result in an apparent negative cooperativity. For typical values of L and c (e.g., 100 000 and 0.001) most terms in eq A8 drop out, resulting in

$$-[H]^2 + 20[H] + 10 = 0 \quad (A9)$$

According to this equation the apparent negative cooperativity will occur for values of H above approximately 20. For values of H below 20, which includes the original MWC model where $H = 0$ (and for all choices of L and c), only positive cooperativity is possible.

References

Bonaventura, C., Bonaventura, J., & Brouwer, M. (1982) *Invertebrate Oxygen-Binding Proteins* (Lamy, J., & Lamy, J., Eds.) pp 677–691, Marcel Dekker, New York.

Brouwer, M., Bonaventura, C., & Bonaventura, J. (1977) *Biochemistry 16*, 3897–3902.

Brouwer, M., Bonaventura, C., & Bonaventura, J. (1978) *Biochemistry 17*, 2148–2154.

Brouwer, M., Bonaventura, C., & Bonaventura, J. (1982a) *Physiology and Biology of Horseshoe Crabs* (Bonaventura, J., Bonaventura, C., & Tesh, S., Eds.) pp 231–256, Alan R. Liss, New York.

Brouwer, M., Bonaventura, C., & Bonaventura, J. (1982b) *Biochemistry 21*, 2529–2538.

Brouwer, M., Bonaventura, C., & Bonaventura, J. (1983) *Biochemistry 22*, 4713–4723.

Coletta, M., Di Cera, E., Brunori, M. (1986) *Invertebrate Oxygen Carriers* (Linzen, B., Ed.) pp 375–381, Springer-Verlag, Heidelberg.

Decker, H., Savel, A., Linzen, B., & van Holde, K. E. (1983) *Life Chem. Rep. 1*, 251–256.

Decker, H., Robert, C. H., & Gill, S. J. (1986) *Invertebrate Oxygen Carriers* (Linzen, B., Ed.) pp 383–388, Springer-Verlag, Heidelberg.

Gaykema, W. P. J., Volbeda, A., & Hol, W. G. J. (1986) *J. Mol. Biol. 187*, 255–275.

Imai, K. (1981) *Methods Enzymol. 76*, 438–449.

Imai, K. (1982) *Allosteric Effects in Haemoglobin*, Cambridge, New York.

Johnson, B. A. (1984) Ph.D. Dissertation, Duke University.

Johnson, B. A. (1987) *J. Comp. Physiol. 157*, 501–509.

Johnson, B. A., Bonaventura, C., & Bonaventura, J. (1984) *Biochemistry 23*, 872–878.

Johnson, M. L., & Ackers, G. K. (1982) *Biochemistry 21*, 201–211.

Johnson, M. L., Correia, J. J., Yphantis, D. A., Halvorsen, H. R. (1981) *Biophys. J. 36*, 575–588.

Kotani, M. (1968) *Suppl. Prog. Theor. Phys.*, 233–241.

Mannervik, B. (1982) *Methods Enzymol. 87*, 370–390.

Mason, R. P., Mangum, C. P., & Godette, G. (1983) *Biol. Bull. (Woods Hole, Mass.) 164*, 104–123.

Miller, K., & van Holde, K. E. (1974) *Biochemistry 13*, 1668–1674.

Mills, F. C. (1978) Ph.D. Thesis, University of Virginia.

Minton, A. P., & Imai, K. (1974) *Proc. Natl. Acad. Sci. U.S.A. 71*, 1418–1421.

Monod, J., Wyman, J., & Changeux, J.-D. (1965) *J. Mol. Biol. 12*, 88–118.

Perutz, M. F. (1979) *Annu. Rev. Biochem. 48*, 327–386.

Richey, B., Decker, H., & Gill, S. J. (1985) *Biochemistry 24*, 109–117.

Solomon, E. I. (1981) *Copper Proteins* (Spiro, T. G., Ed.) pp 41–108, Wiley, New York.

van Holde, K. E., & Miller, K. I. (1982) *Q. Rev. Biophys. 15*, 1–129.